Scientia Iranica (2024) 31(2), 161–173

Sharif University of Technology
Scientia Iranica
Transactions D: Computer Science & Engineering and Electrical Engineering
https://scientiairanica.sharif.edu

Performance improvement of a system-level harmonic using a harmonic power flow controller

R. Mehri[a], H. Mokhtari[b,*], and M.R. Zolghadri[b]

a. *Department of Engineering, College of Electrical Engineering, Science and Research Branch, Islamic Azad University, Tehran, Iran.*
b. *Department of Electrical Engineering, Sharif University of Technology, Tehran, Iran.*

Received 24 August 2021; received in revised form 26 December 2021; accepted 14 March 2022

KEYWORDS
Harmonic voltage control;
Current harmonic flow;
HPFC;
ZAPI;
MAPI;
IZAPI;
IMAPI;
Harmonic power loss control.

Abstract. Penetration of harmonics from downstream low voltage networks and resonance phenomenon has caused the level of harmonics to increase in transmission networks. Compensation for these harmonics at high voltage levels is neither recommended nor cost-effective. This is due to the fact that there is no single large non-linear load that causes these harmonics, yet filtering at low voltage non-linear load sites cannot completely compensate the harmonics, and the remaining harmonics at standard levels still flow into the upstream networks. The idea of controlling harmonics at a medium/high voltage level caused by the remaining harmonics flown from low voltage networks and possibly amplified by resonance conditions with the use of a series of active power filters has been proposed by the authors in a published work. Since this application of a series of active filters was new, it was preferred to assign a new name for such device, i.e., harmonic power flow controller or simply HPFC. This work looks into the control strategies applicable to an HPFC in more detail. The shortcomings of the previous methods are now removed, resulting in better performance for an HPFC.

1. Introduction

Filtering at low voltage levels and at the non-linear load sites has been the most common solution to mitigate harmonics and prevent them from entering upstream medium/high voltage networks [1–6]. However, for several reasons, this filtering cannot completely absorb the harmonics [7,8]. One can consider harmonics caused by distributed low-power loads, such as residential customers, which do not normally use any filtering equipment. It is also worth mentioning that all filtering techniques limit the levels of harmonics to the limits specified by standards such as IEEE-519. On the other hand, in several cases, it is observed the remaining harmonics at low voltage levels penetrate into the medium/high voltage networks and are amplified by resonance conditions.

In many cases, mitigating the remaining harmonics at a medium/high voltage network is not easily possible due to the fact that the source of harmonics is not located at medium/high voltage, and there is no single large non-linear load at which site a filter can be installed. To tackle the issue, the authors proposed a new method of controlling harmonic currents at medium/high voltage networks by the use of Series

*. *Corresponding author. Tel.: +98 21 66165962*
E-mail addresses: Reza-mehri@iauh.ac.ir (R. Mehri); mokhtari@sharif.edu (H. Mokhtari); zolghadr@sharif.edu (M.R. Zolghadri)

doi: 10.24200/sci.2022.58462.5753

Active Power Filters (SAPFs) [9,10]. The main idea in Ref. [10] is to control the flow of harmonic currents and redirect them into paths, which will result in a better harmonic profile. In this method, the SAPF injects a harmonic voltage term into a line to create a change in harmonic flow [10]. This action can be compared to what a phase shifter does at the main frequency. Since the task performed by the SAPF in this application is different from what has been considered for a SAPF, the authors preferred to consider a new name for SAPF in this task, i.e., harmonic power flow controller or simply HPFC.

Principles of operation and the proof of concept of the HPFC were presented in [10]. Two primary control methods were also introduced in [10] for the operation of an HPFC. This work is a continuation of [10]. The authors in the current paper have tried to improve the control methods of an HPFC and alleviate the shortcomings of the proposed control strategies. In order to have a complete work, the basics of the device's principles of operation are again summarized in this work, and therefore, some of the figures are similar to those of in Ref. [10].

The control methods proposed in [10] are named Zero Active Power Injection (ZAPI) and Minimum Apparent Power Injection (MAPI) control methods. The improved methods in this work are named Improved ZAPI or IZAPI and Improved MAPI or IMAPI.

The structure of this work is as follows. In Section 2, the structure and principles of operation of the HPFC are reviewed. ZAPI and MAPI control methods are briefly discussed, and their shortcomings are described. Section 3 presents the IZAPI and IMAPI control methods. The performance of the proposed new control strategies is tested through simulation on the IEEE 14-bus test bed. Section 4 proposes a new control method based on a cost-optimization technique. In Section 5, an HPFC is designed to address a real harmonic problem in Iran's northwest HV transmission network. Finally, Section 6 summarizes the conclusions.

2. Structure and control of HPFC

Figure 1(a) shows a circuit diagram of an HPFC in a simple network that is composed of a Voltage Source Converter (VSC), an energy storage element, and a series transformer [10]. In this configuration, a voltage harmonic term is created by the VSC and injected into the grid through the series transformer.

Depending on the control strategy, an HPFC may need to exchange active/reactive power with the grid. This property can be compared to that of a Dynamic Voltage Restore (DVR) [11–15]. If an active power exchange occurs, an energy source at the DC link is required (Figure 1(b)) [13].

For conceptual and steady-state analysis, an HPFC is modeled as a series harmonic voltage source whose amplitude and angle are controllable [16]. Figure 2 shows an equivalent model of the HPFC. In this model, the amplitude and the angle of line current harmonic (I_h) can be controlled by the amplitude (V_{hpfc}) and angle (θ_h) of the HPFC output [10].

The same as a DVR [11–15], the size and complexity of an HPFC depends on the magnitude and phase angle of the series injected harmonic voltage. Therefore, several strategies of harmonic voltage injection can be considered, and depending on the active/reactive/harmonic power exchange between the line and the HPFC, the structure and size of the HPFC will change.

In [10], two control methods, MAPI and ZAPI, were proposed. In Figure 3, the MAPI control vector diagram of an HPFC in a sample line is shown. In

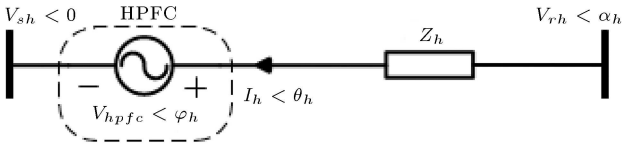

Figure 2. HPFC equivalent model with no active power exchange with the network [10].

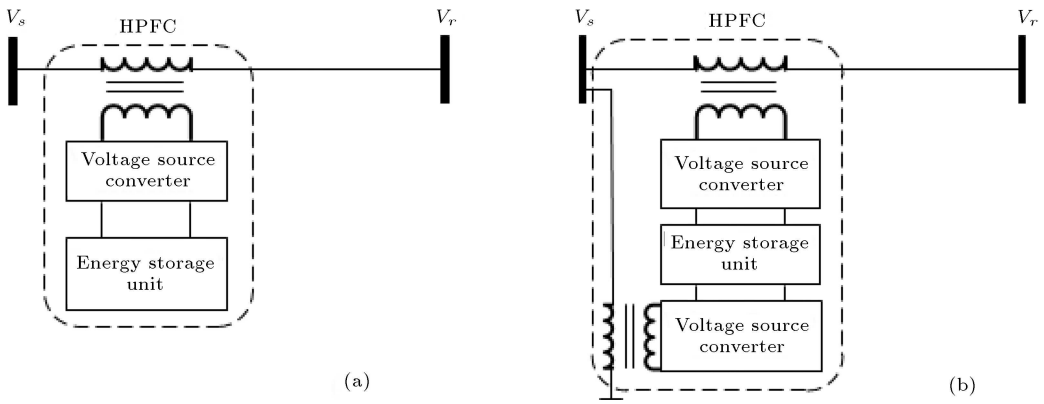

Figure 1. HPFC circuit diagram on a sample line (a) without active power exchange and (b) with active power exchange [10].

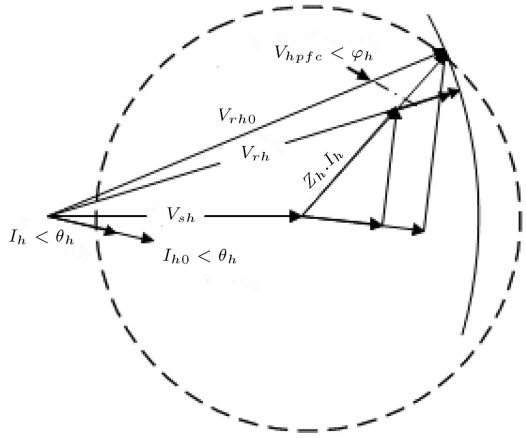

Figure 3. HPFC controlling vector diagram (V_{rh} is constant) in the MAPI control method [13].

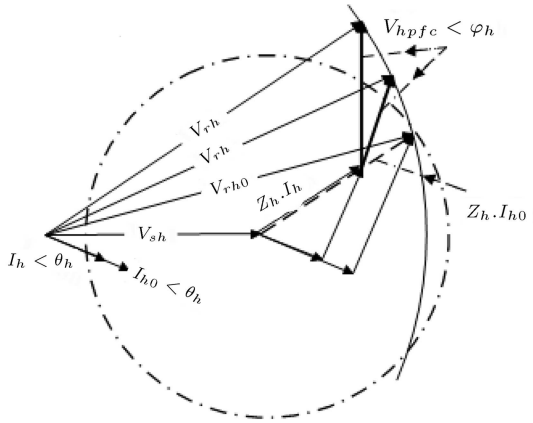

Figure 4. HPFC controlling vector diagram (V_{rh} is constant) in the ZAPI control method [13].

this diagram, Z_h is the harmonic impedance of the line in which the HPFC is installed. V_{sh}, V_{rh0}, and I_{h0} are bus-side, line-side harmonic voltage, and the line harmonic current, respectively, before using the HPFC. By using the HPFC, the injected harmonic term of V_{hpfc} will change V_{rh0}, I_{h0} to V_{rh}, I_h.

In the MAPI control method, the injected harmonic voltage V_{hpfc} is such that the rating of the HPFC is minimized. To achieve this, the injected harmonic voltage (V_{hpfc}) must be as low as possible. This results in an injection signal in phase with V_{rh}.

In the ZAPI control method, the HPFC-injected harmonic voltage (V_{hpfc}) is perpendicular to the harmonic current, as shown in Figure 4. Therefore, no harmonic power is exchanged between the HPFC and the network.

MAPI and ZAPI methods are inaccurate methods because they control the HPFC by sampling, sending, and receiving HPFC line parameters. In the MAPI method, the HPFC apparent power is not precisely minimized, and in the ZAPI method, the HPFC active power is not exactly zero because injecting a series harmonic voltage will also change the bus side harmonic voltage.

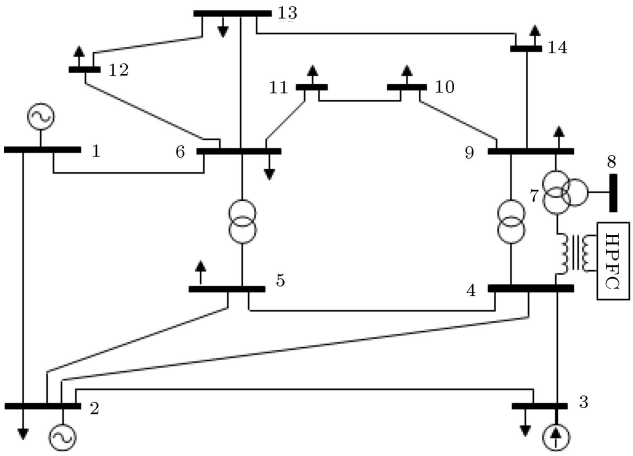

Figure 5. The 14 bus-bar test system, an HPFC, and the harmonic source [8].

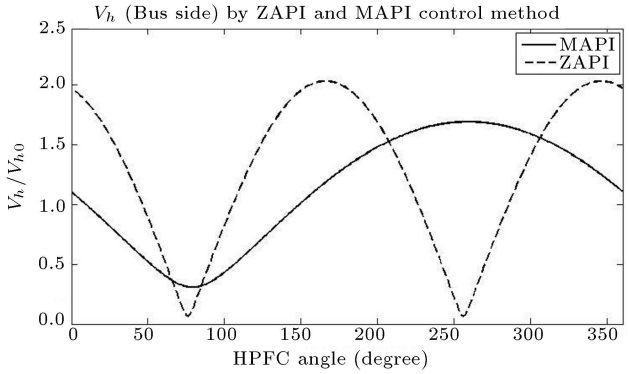

Figure 6. Harmonic voltage variation of bus side respect to no-HPFC in MAPI/ZAPI control method when HPFC is located between buses 4 and 7.

To show this concept, an HPFC is tested on the IEEE 14-busbar test system [17,18]. Figure 5 shows the system under study. The study is performed for only the 5th harmonic, which is normally the dominant harmonic in power networks.

As Figure 5 shows, an HPFC is placed in the feeder between buses 4 and 7. Table 1 lists the values of the linear and non-linear loads in the system.

The HPFC injects a 5th harmonic voltage in the feeder between buses 4 and 7, and the outcome is studied. The angle of the injected voltage is changed from 0 to 360°.

Figure 6 shows the 5th harmonic voltage variation at the bus side (bus 7) in the ZAPI/MAPI control method as the result of the HPFC operation. The study shows that the harmonic voltage of this busbar changes by the injected harmonic voltage by the HPFC. Therefore, it is necessary to keep this voltage, V_{sh}, unchanged.

3. IZAPI and IMAPI control methods

Using the sending/receiving line parameters results in

Table 1. Specification of the loads under study [8].

Bus no.	Static load spec.		5th order harmonic current	
	P (MW)	Q (MVar)	Mag. (%)	Angle (degree)
4	47.79	–3.9	10	5
5	7.6	1.6	20	10
8	29.5	16.6	20	30
9	29.5	16.6	15	10
10	9	5.8	10	80
11	3.5	1.8	25	50
12	6.1	1.6	20	30
13	13.5	5.8	15	20
14	14.9	5	20	30

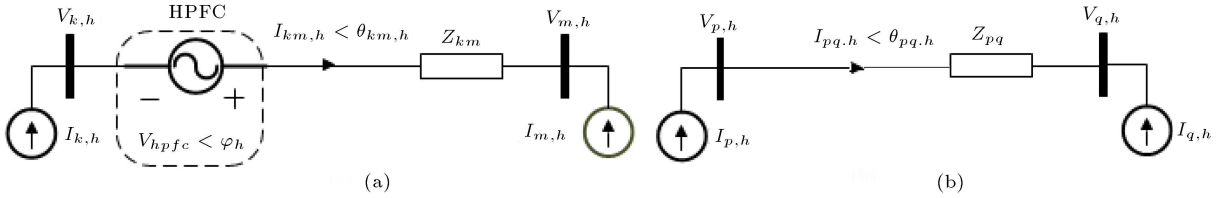

Figure 7. Network model of (a) HPFC on line $k-m$ and (b) Line $p-q$ without HPFC.

accuracy of MAPI/ZAPI methods. In other words, in the MAPI method, the HPFC apparent power is not precisely minimized, and in the ZAPI method, the HPFC active power is not exactly zero.

To increase the accuracy of these methods, it is essential to incorporate other parameters of the network into the HPFC control algorithm. For this purpose, the IMAPI and IZAPI methods are proposed as the improved versions of MAPI and ZAPI.

3.1. IMAPI method

Figure 7 shows an installed HPFC in a typical line, e.g., km. In this figure, V_h (harmonic voltage of network buses) can be calculated as:

$$V_h = V_{h0} - Z_h * Y_{HPFC,h} * V_{HPFC,h}, \tag{1}$$

$$V_{h0} = Z_h * I_{h0}, \tag{2}$$

where V_{h0} is the initial harmonic voltage vector without HPFC; I_{h0} the initial harmonic current vector without HPFC; Z_h the impedance matrix of the network, as calculated by Eqs. (3) and (4) are shown in Box I.

The complex, active/reactive, and apparent powers of the HPFC can be calculated as follows:

$$\overline{S_{HPFC}} = \left[V_{HPFC,h} * \overline{I_{km,h}}\right] = P_{HPFC} + j * Q_{HPFC}, \tag{5}$$

$$P_{HPFC} = |V_{HPFC,h}| * |I_{km,h0}| * \cos\left(\theta_{HPFC,h} - \theta_{I_{km,h0}}\right) + |V_{HPFC,h}|^2 * |A_{km,h}| * \cos\left(\theta_{A_{km,h}}\right), \tag{6}$$

$$Q_{HPFC} = |V_{HPFC,h}| * |I_{km,h0}| * \sin\left(\theta_{HPFC,h} - \theta_{I_{km,h0}}\right) - |V_{HPFC,h}|^2 * |A_{km,h}| * \sin\left(\theta_{A_{km,h}}\right), \tag{7}$$

$$|S_{HPFC}| = (P_{HPFC}{}^2 + Q_{HPFC}{}^2)^{(1/2)} = V_{HPFC} * [|I_{km,h0}|^2 + |V_{HPFC,h}|^2 * |A_{km,h}|^2 + 2|I_{km,h0}| * |V_{HPFC,h}| * |A_{km,h}| * Cos(\theta_{A_{km,h}} + \theta_{HPFC,h} - \theta_{I_{km,h0}}]^{(1/2)}. \tag{8}$$

To minimize the apparent power (HPFC capacity), the derivative of Eq. (8) with respect to $\theta_{HPFC,h}$ is calculated and set to zero, i.e.:

$$Z_h = \begin{bmatrix} Z_{11,h} & \cdots & Z_{1p,h} & Z_{1q,h} & & Z_{1m,h} & \cdots & Z_{1k,h} & \cdots & Z_{1n,h} \\ \vdots & \cdots & \vdots & \vdots & & \vdots & \cdots & \vdots & \cdots & \vdots \\ Z_{p1,h} & \cdots & Z_{pp,h} & Z_{pq,h} & \cdots & Z_{pm,h} & \cdots & Z_{pk,h} & \cdots & Z_{pn,h} \\ \vdots & \cdots & \vdots & \vdots & & \vdots & \cdots & \vdots & \cdots & \vdots \\ Z_{q1,h} & \cdots & Z_{qp,h} & Z_{qq,h} & \cdots & Z_{qm,h} & \cdots & Z_{qk,h} & \cdots & Z_{qn,h} \\ & & \vdots & & \ddots & & & \vdots & & \\ Z_{m1,h} & \cdots & Z_{mp,h} & Z_{mq,h} & & Z_{mm,h} & \cdots & Z_{mk,h} & \cdots & Z_{mn,h} \\ \vdots & \cdots & \vdots & \vdots & & \vdots & \cdots & \vdots & \cdots & \vdots \\ Z_{k1,h} & \cdots & Z_{kp,h} & Z_{kq,h} & \cdots & Z_{km,h} & \cdots & Z_{kk,h} & \cdots & Z_{kn,h} \\ \vdots & \cdots & \vdots & \vdots & & \vdots & \cdots & \vdots & \cdots & \vdots \\ Z_{n1,h} & \cdots & Z_{np,h} & Z_{nq,h} & \cdots & Z_{nm,h} & \cdots & Z_{nk,h} & \cdots & Z_{nn,h} \end{bmatrix}, \tag{3}$$

$$Y_{HPFC,h} = \begin{bmatrix} 0 \\ \vdots \\ +Y_{km,h} \\ \vdots \\ -Y_{km,h} \\ \vdots \\ 0 \end{bmatrix}, V_h = \begin{bmatrix} V_{1,h} \\ \vdots \\ V_{p,h} \\ \vdots \\ V_{q,h} \\ \vdots \\ V_{m,h} \\ \vdots \\ V_{k,h} \\ \vdots \\ V_{n,h} \end{bmatrix}, I_h = \begin{bmatrix} I_{1,h} \\ \vdots \\ I_{p,h} \\ \vdots \\ I_{q,h} \\ \vdots \\ I_{m,h} \\ \vdots \\ I_{k,h} \\ \vdots \\ I_{n,h} \end{bmatrix}. \tag{4}$$

Box I

$$\frac{d|S_{HPFC}|}{d\theta_{HPFC,h}} = K_{costant} * \Big\{ {V_{HPFC}}^2 * [2|I_{(km,h0)}| * |V_{HPFC,h}| * |A_{km,h}| * \sin(\theta_{A_{km,h}} + \theta_{HPFC,h} - \theta_{I_{km,h0}})] \Big\} = 0. \tag{9}$$

By solving Eq. (9), the angle of the HPFC for minimizing the HPFC capacity can be derived as Eq. (10):

$$\theta_{HPFC,h} = k\pi \pm \left(\theta_{I_{km,h0}} - \theta_{A_{km,h}}\right). \tag{10}$$

This relation shows that the HPFC angle depends on the HPFC line current angle and the angle of an equal impedance $A_{km,h}$ (This value is constant).

To study the effect of the IMAPI Control method, an HPFC is placed in the feeder between buses 4 and 7 of the IEEE 14-busbar test system. Figure 8 shows the harmonic apparent, active, and reactive powers of the HPFC and the optimum angle of the HPFC. Figure 9 shows the harmonic voltages at all buses with and without the HPFC. It can be seen from Figure 9 that the harmonic voltage values have changed by the HPFC.

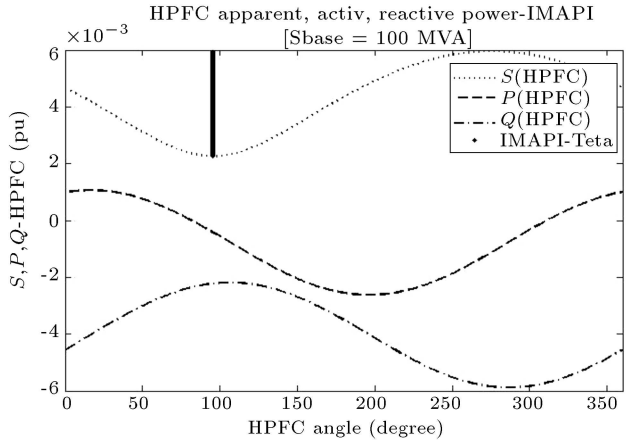

Figure 8. Harmonic apparent, active, and reactive power of the HPFC in IMAPI control method (Bold line: Optimum angle of the HPFC).

3.2. IZAPI method

The harmonic active power of the HPFC can be

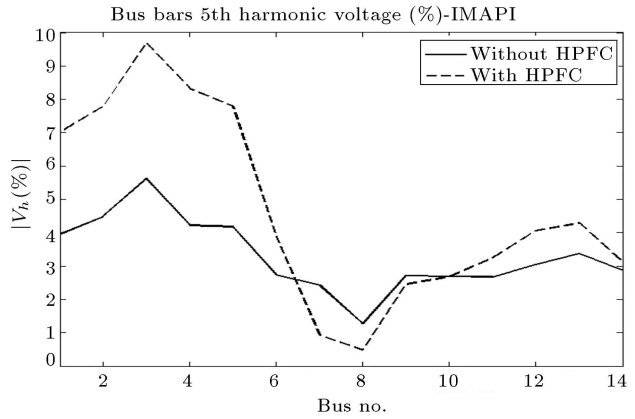

Figure 9. Harmonic voltage of bus-bars with and without HPFC in IMAPI control method.

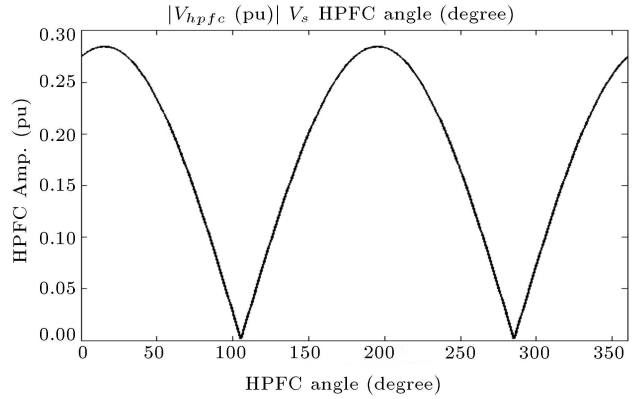

Figure 10. Locus of HPFC output amplitude/angle in IZAPI control method.

calculated by Eq. (6). In the IZAPI control method, no harmonic power is exchanged between the HPFC and the network.

The HPFC harmonic current and voltage magnitude are obtained from the following equations:

$$|I_{km,h0}| * \cos\left(\theta_{HPFC,h} - \theta_{I_{km,h0}}\right) + |V_{HPFC,h}| * |A_{km,h}| * \cos\left(\theta_{A_{km,h}}\right) = 0, \quad (11)$$

$$|V_{HPFC,h}| = -\left\{\frac{|I_{km,h0}|}{|A_{km,h}|}\right\} * \left\{\frac{\cos\left(\theta_{HPFC,h} - \theta_{I_{km,h0}}\right)}{\cos\left(\theta_{A_{km,h}}\right)}\right\}. \quad (12)$$

Figure 10 shows the locus of the amplitude of the HPFC versus its angle in the IZAPI control method (HPFC is installed in lines 4–7). This figure shows that for the IZAPI control method, the amplitude and the angle of the HPFC depend on each other.

Figure 11 shows the harmonic apparent, reactive, and active power of the HPFC in the IZAPI control method. Simulation results show that by using this method, no harmonic active power is exchanged between the HPFC and the network.

Figure 12 shows the HPFC line harmonic current variations and the HPFC harmonic reactive power versus the HPFC amplitude in the IZAPI control method. This figure shows that the HPFC amplitude is limited by the level of harmonic current control and the HPFC capacity.

4. Cost function control algorithm method

In previous subsections, IMAPI/IZAPI methods were considered to control the HPFC parameters based on the bus's harmonic voltages and series line/transformer harmonic current values. In these methods, the injected harmonic voltage is such that the rating of the HPFC is minimized or no harmonic power is exchanged between the HPFC and the network. In these methods, there is no control over the network parameters, such as harmonic power losses and other bus-bar harmonic voltage values. It is essential to define a cost function for an HPFC to control the network parameters, such as harmonic power losses and harmonic voltage variations.

4.1. Harmonic voltage minimization

Harmonic voltage at bus j can be determined as:

$$V_{j,h} = V_{j,h0} + (Z_{jk,h} - Z_{jm,h}) * Y_{km,h} * V_{HPFC,h} = V_{j,h0} + C_{j,h} * V_{HPFC,h}, \quad (13)$$

where $C_{j,h}$ is:

$$C_{j,h} = (Z_{jk,h} - Z_{jm,h}) * Y_{km,h}. \quad (14)$$

For this purpose, the cost function is defined as follows:

$$\begin{aligned} Cost\ function &= \sum_{j=1}^{M} \left(|V_{j,h}|^2 - |V_{j,h0}|^2\right) * K_j \\ &= \sum_{j=1}^{M} \Bigg(K_j * \Big\{|V_{j,h0}|^2 + |C_{j,h}|^2 * |V_{HPFC,h}|^2 + 2 * |V_{j,h0}| * |C_{j,h}| * |V_{HPFC,h}| * \cos\Big(\theta_{HPFC,h} + \theta_{C_{j,h}} - \theta_{V_{j,h0}}\Big)\Big\} \\ &\quad - |V_{j,h0}|^2\Bigg) \sum_{j=1}^{M} \Bigg(K_j * \Big\{|C_{j,h}|^2 * |V_{HPFC,h}|^2 + 2 * |V_{j,h0}| * |C_{j,h}| \end{aligned}$$

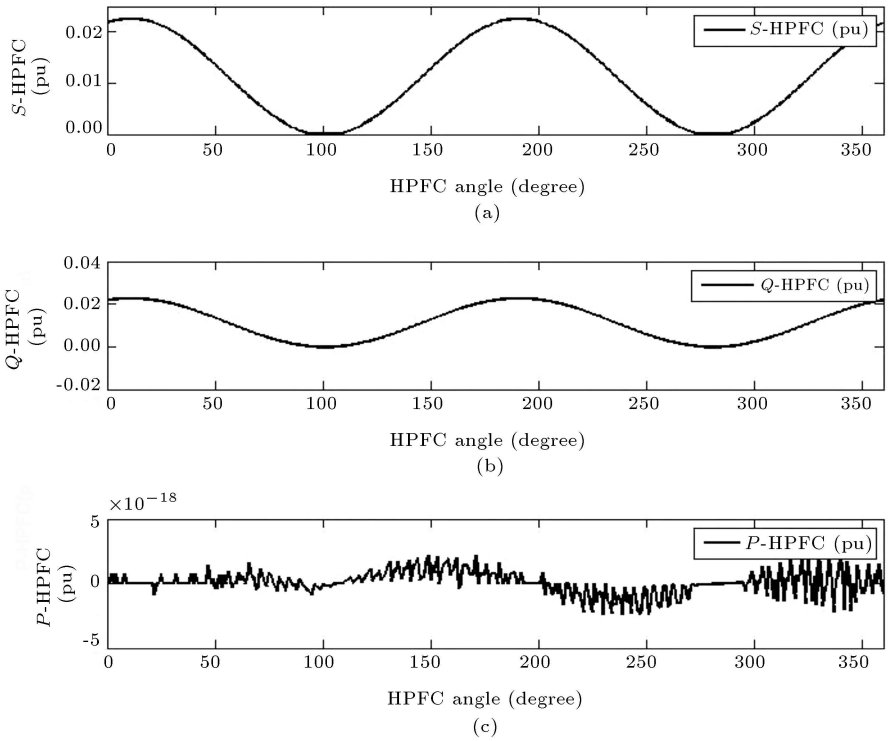

Figure 11. Harmonic apparent (a), reactive (b), and active (c) power of HPFC in the IZAPI control method.

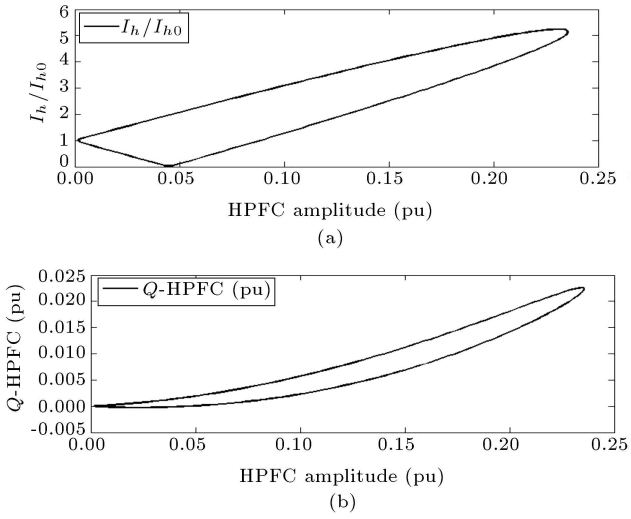

Figure 12. HPFC line harmonic current variation (a) and HPFC harmonic reactive power and (b) versus HPFC value in IZAPI control method (I0 is HPFC current before HPFC installation).

$$* |V_{HPFC,h}| * \cos\left(\theta_{HPFC,h} + \theta_{C_j,h} - \theta_{V_{j,h0}}\right)\Big\}\Big)\theta_{V_{j,h0}} =< V_{j,h0}, \theta_{HPFC,h} =< V_{HPFC,h}, \theta_{C_j,h} =< C_{j,h}, \quad (15)$$

where K_j is the weighting factor of the jth bus harmonic voltage variation.

Table 2. HPFC angle for minimum harmonic voltage.

Line	$\theta_{HPFC,h}$	Line	$\theta_{HPFC,h}$
4–7	256.98°	7–9	76.63°
5–6	276.57°	9–10	262.36°
6–11	107.71°	9–14	253.44°
7–8	256.77°	10–11	280.91°

In the cost function, all the parameters are constant values, and the HPFC angle is controlled to optimize the cost function. To achieve this, it is necessary to solve the following equation:

$$\frac{d\ cost\ function}{d\theta_{HPFC,h}} = \sum_{j=1}^{M}\Bigg(-2 * K_j * \Big\{|V_{j,h0}| * |C_{j,h}| * |V_{HPFC,h}| * \sin\Big(\theta_{HPFC,h} + \theta_{C_j,h} - \theta_{V_{j,h0}}\Big)\Big\}\Bigg) = 0. \quad (16)$$

To investigate the effect of this control method, an HPFC is installed in different lines in the IEEE 14-bus test system. Table 2 shows the HPFC angle to minimize harmonic voltage by installing the HPFC at different lines.

Simulations show that when the voltage harmonic decreases, harmonic power losses will increase by about

Table 3. HPFC angle for minimum harmonic power loss.

Line	$\theta_{HPFC,h}$	$P_{Loss,h}$ (pu)	Line	$\theta_{HPFC,h}$	$P_{Loss,h}$ (pu)
4–7	75.97°	0.1898	7–9	242.11°	0.2097
5–6	257.4°	0.1894	9–10	94.96°	0.2188
6–11	235.9°	0.2144	9–14	315.18°	0.2061
7–8	72.31°	0.1831	10–11	60.41°	0.2155

17.9% when the HPFC is installed in lines 5–6. Therefore, for the optimum control of harmonic voltages, it is necessary to consider harmonic power losses in the cost function as well.

4.2. Harmonic power loss minimization

Harmonic power losses can be determined as follows:

$$P_{Loss,h} = 3 * \sum_{j=1}^{M} \left(R_{j,h} * |I_{j,h}|^2 \right), \tag{17}$$

$$I_{pq,h} = \left(V_{p,h} - V_{q,h} \right) / Z_{pq,h}, \tag{18}$$

$$I_{km,h} = \left(V_{k,h} - V_{m,h} - V_{HPFC,h} \right) / Z_{km,h}, \tag{19}$$

where $I_{pq,h}$ and $I_{km,h}$ are the harmonic currents of the lines pq and km, respectively.

$V_{p,h}$ and $V_{q,h}$ (harmonic voltage of buses p and q) can be determined as:

$$V_{p,h} = V_{p,h0} + (Z_{pk,h} - Z_{pm,h}) * Y_{km,h} * V_{HPFC,h}, \tag{20}$$

$$V_{q,h} = V_{q,h0} + (Z_{qk,h} - Z_{qm,h}) * Y_{km,h} * V_{HPFC,h}. \tag{21}$$

Finally, the cost function (harmonic power losses) is defined as:

$$Cost\ function = P_{Loss,h} = P_{Loss,h0} + K_{A,h} * |V_{HPFC,h}|^2 + K_{B,h} * |V_{HPFC,h}|, \tag{22}$$

where $P_{Loss,h0}$, $K_{A,h}$, $K_{B,h}$ are as follows:

$$K_{A,h} = 3 * \sum_{j=1}^{M} \left(R_{j,h} * |A_{j,h}|^2 \right), \tag{23}$$

$$K_{B,h} = \sum_{j=1}^{M} 6 \Big(R_{j,h} * |I_{j,h0}| * |A_{j,h}| * \cos\left(\theta_{I_{j,h0}} - \theta_{HPFC,h} - \theta_{A_{j,h}} \right) \Big), \tag{24}$$

$$\theta_{I_{j,h0}} =< I_{j,h0}, \theta_{HPFC,h} =< V_{HPFC,h}, \theta_{A_{j,h}} =< A_{n,h}, \tag{25}$$

where $A_{j,h}$ is a constant value that depends on the line impedances, which is calculated using Eq. (25):

$$A_{j,h} = ((Z_{pm,h} - Z_{pk,h}) - (Z_{qm,h} - Z_{qk,h})) * Y_{mk,h} / Z_{j,h}. \tag{26}$$

If the line is an HPFC-installed line, $A_{j,h}$ must be determined from the following relation:

$$A_{j,h} = (1 + Y_{mk,h} * (Z_{mm,h} + Z_{kk,h} - 2 * Z_{mk,h})) / Z_{j,h}. \tag{27}$$

In the cost function, all the parameters are constant values, and the HPFC angle is changed to optimize the cost function. To minimize the harmonic power, Eq. (27) must be met:

$$\frac{d\ cost\ function}{d\theta_{HPFC,h}} = |V_{HPFC,h}| * \frac{K_{B,h}}{d\theta_{HPFC,h}} = 6 * |V_{HPFC,h}| * \sum_{j=1}^{M} \Big(R_{j,h} * |I_{j,h0}| * |A_{j,h}| * \sin\left(\theta_{I_{j,h0}} - \theta_{HPFC,h} - \theta_{A_{j,h}} \right) \Big) = 0. \tag{28}$$

Because of the complexity of Eq. (27), the bisection method is used to find $\theta_{HPFC,h}$. Table 3 shows the HPFC angle to minimize the harmonic power losses by installing an HPFC in different lines.

Simulation shows when harmonic power losses decrease, harmonic voltages will increase or decrease when the HPFC is located in lines 5–6 (Figure 13).

4.3. Harmonic voltage and power loss minimization

Because of the dependency of harmonic voltages and harmonic power losses, it is essential to define a complete cost function that includes both quantities. This cost function is defined as:

$$Cost\ function = Cost\ function\left(\Delta V_h^2 \right) + Cost\ function\ (P_{Loss,h}) = \sum_{j=1}^{N} \Big(|V_{j,h}|^2$$

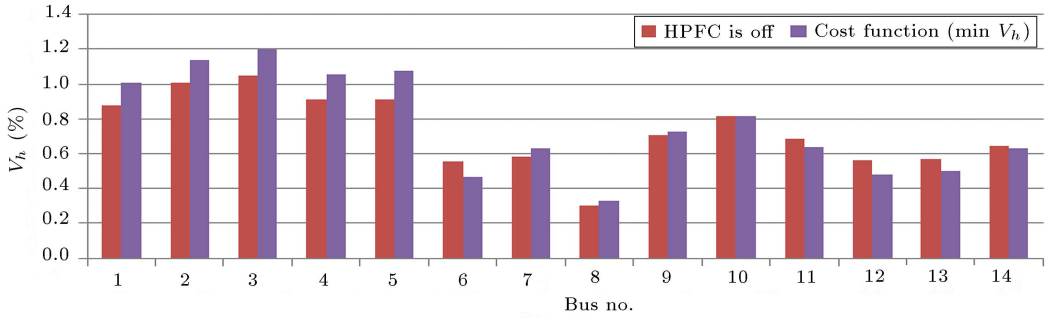

Figure 13. Effect of harmonic voltage minimization algorithm control on the voltage harmonic of different buses when the HPFC is located in lines 5–6.

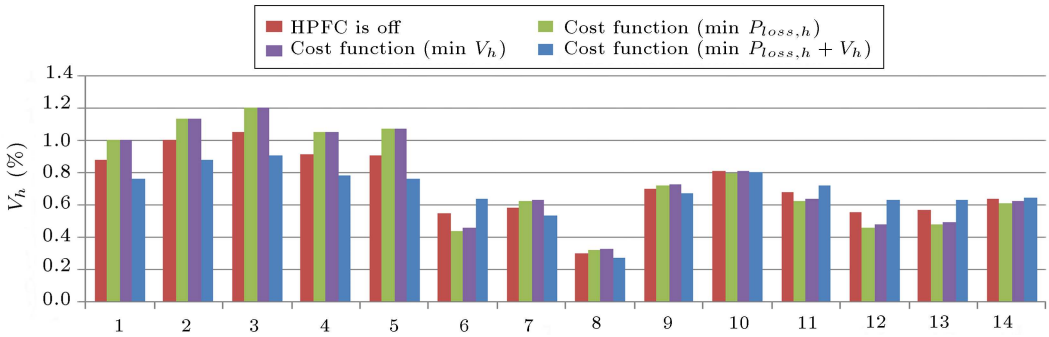

Figure 14. Effect of HPFC cost function algorithm control on voltage harmonic of different buses when the HPFC is located in lines 5–6.

$$-|V_{j,h0}|^2\Big)*K_j + P_{Loss,h0} + K_{A,h}$$

$$*|V_{HPFC,h}|^2 + K_{B,h} * |V_{HPFC,h}|\,. \qquad (29)$$

To minimize the cost function, it is necessary to solve the following equation, which can be done using the bisection method:

$$\frac{d\ cost\ function}{d\theta_{HPFC,h}} = \sum_{j=1}^{N}\Bigg(-2 * K_j * \Big\{|V_{j,h0}| * |C_{j,h}|$$

$$* |V_{HPFC,h}| * \sin\left(\theta_{HPFC,h} + \theta_{C_{j,h}} - \theta_{V_{j,h0}}\right)\Big\}\Bigg)$$

$$+ 6 * |V_{HPFC,h}| * \sum_{j=1}^{M}\Big(R_{j,h} * |I_{j,h0}| * |A_{j,h}|$$

$$* \sin\left(\theta_{I_{j,h0}} - \theta_{HPFC,h} - \theta_{A_{j,h}}\right)\Big) = 0. \qquad (30)$$

Table 4 shows the HPFC angle for minimizing the cost function by installing an HPFC in different lines. Simulation shows that by using this cost function, the harmonic voltage (Figure 14) and harmonic power losses (Figure 15) can be reduced simultaneously when the HPFC is located in lines 5–6.

Table 4. HPFC angle for harmonic voltage and power loss minimization.

Line	$\theta_{HPFC,h}$	Line	$\theta_{HPFC,h}$
4–7	256.7°	7–9	75.42°
5–6	288.41°	9–10	265.62°
6–11	88.59°	9–14	221.15°
7–8	256.57°	10–11	266.75°

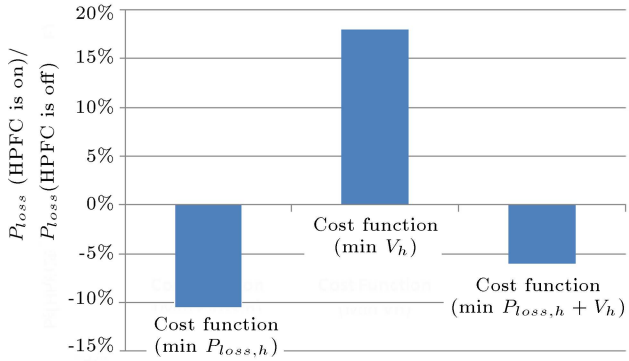

Figure 15. Effect of different cost function algorithm controls on active harmonic power losses of network variation when the HPFC is located in lines 5–6.

5. Simulation for a real network

In this section, the effect of the HPFC is evaluated in a real network, i.e., Iran's northwest transmission system. Harmonic measurements have been performed

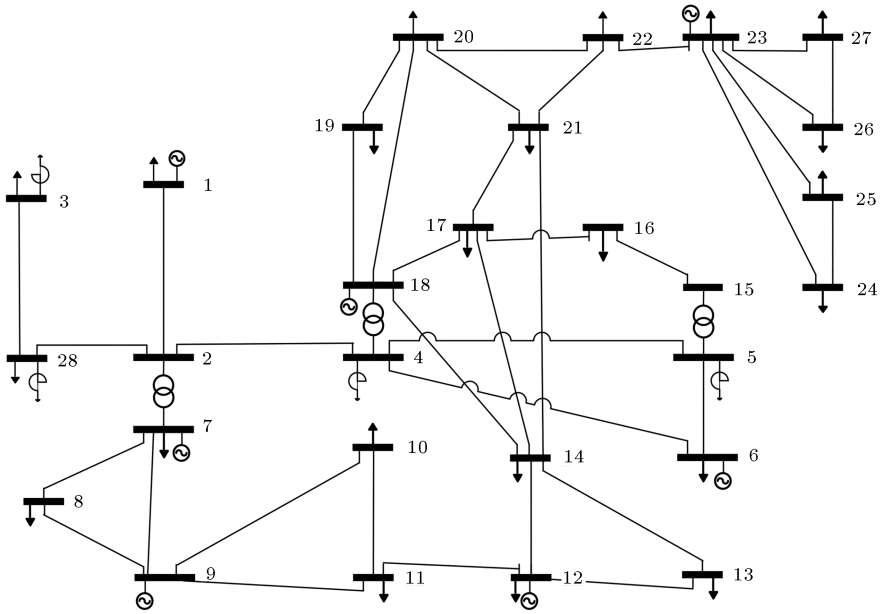

Figure 16. Iran north-west transmission system single-line diagram.

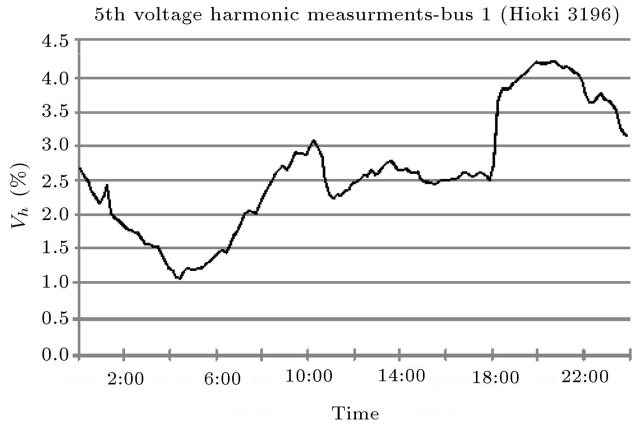

Figure 17. 5th harmonic voltage measurements at bus 1.

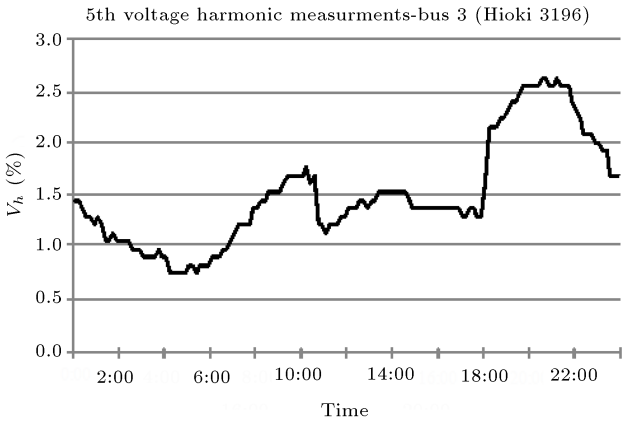

Figure 18. 5th harmonic voltage measurements at bus 3.

at different locations in Iran's NW transmission system (Figure 16) using the HIOKI-3196 power quality analyzer. Figures 17 and 18 show the harmonic measurement at buses 1 and 3 for a one-day period, which is recorded by 10-minute sampling intervals. Figure 19 shows the harmonic voltage value at all buses at about 20:00 o'clock. As can be seen, the 5th harmonic level is above the IEEE 519 Std. limit (i.e., 1%) during most of the measurement period. The objective, in this case, is to use an HPFC to change the harmonic impedance and accordingly alter harmonic flows such that the 5th harmonic level at bus 3 is decreased.

To design the HPFC, the system model must first be derived. The network is modeled at 400 kV and 230 kV voltage levels with 28 buses (Figure 16).

The harmonic voltage at bus No. 3 is 4.3%, which has caused complications in the network. To overcome the complications, the harmonic voltage needs to be decreased to a level below 2% (IEC 61000-2).

Table 5 shows the HPFC signal magnitude and angle using IZAPI and IMAPI control methods and minimizing the different cost functions by installing an HPFC in an optimum line.

Figure 20 shows the harmonic voltage values of all buses for the control methods and their corresponding injected harmonic voltage given in Table 5. Table 6 summarizes the network harmonic power loss, HPFC exchange apparent, and active and reactive powers.

These simulations indicate that the network parameters cannot be controlled by IZAPI and IMAPI methods alone. The harmonic power loss is increased if the harmonic voltage minimization control method is used. The harmonic voltage of some buses is increased if only the power-loss minimization method is employed. Harmonic voltage and harmonic power losses

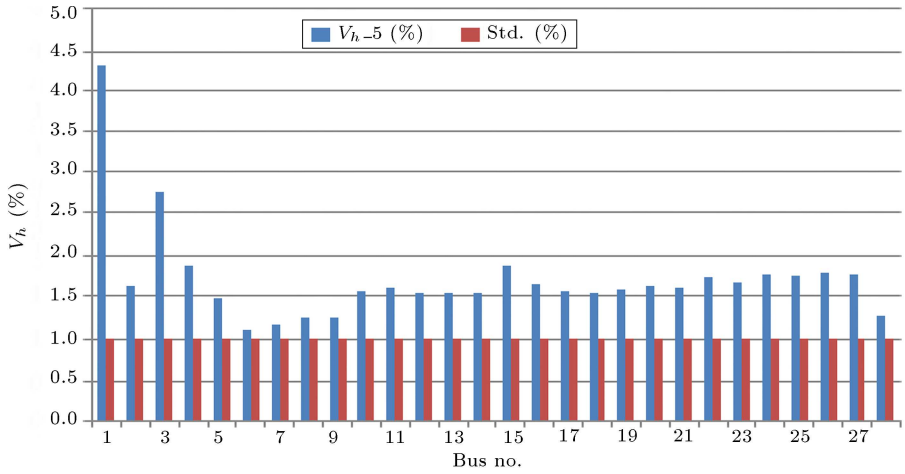

Figure 19. 5th harmonic voltage measurements at all busses.

Table 5. Optimum HPFC angle for harmonic voltage and power loss minimization.

HPFC control method	Line	$\lvert V_{HPFC,h}\rvert$	$\theta_{HPFC,h}$
IZAPI method	2–4	0.0315	208.7°
IMAPI method	2–4	0.0304	37.4°
Harmonic power loss minimization	5–6	0.03	145.7°
Harmonic voltage minimization	2–28	0.03	127.8°
Harmonic voltage and power loss minimization	2–4	0.03	351.4°

Table 6. Total harmonic power and HPFC harmonic apparent, active, and reactive power for different HPFC control methods.

HPFC control method	$P_{Loss,h}$ (kW)	$S_{HPFC,h}$ (kVA)	$P_{HPFC,h}$ (kW)	$Q_{HPFC,h}$ (kVAR)
Without HPFC	522	–	–	–
IZAPI method	782	1005	0	1005
IMAPI method	572	376	367	–82
Harmonic power loss minimization	425	684	510	–455
Harmonic voltage minimization	451	510	–25	–510
Harmonic voltage and power loss minimization	463	490	74	–484

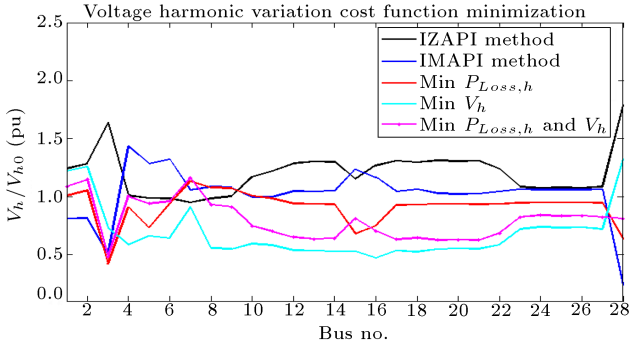

Figure 20. Ratio of harmonic voltage at Iran northwest bus-bars after installation of an HPFC in optimum line with ZAPI, MAPI control methods, and harmonic voltage and power loss control methods.

can be reduced simultaneously if the last proposed method is used.

In Table 6, the exchange power by HPFC and network is shown. By these values, the capacity and structure of HPFC (with and without a power supply) are obtained.

6. Conclusion

In this paper, the performance of a recently introduced harmonic conditioner, i.e., harmonic power flow controller or HPFC, has been improved by introducing new control strategies for the HPFC. It is shown that by employing the IMAPI/IZAPI control methods, one can more effectively reduce the size of the HPFC as compared to the previous MAPI/ZAPI control algorithms. Furthermore, two operating performance parameters, i.e., the harmonic profile of the network and the harmonic losses cost function, are considered and incorporated in the design and control of the HPFC. It is shown that HPFC can effectively achieve a harmonic environment in places where no absorption harmonic filter can be installed.

References

1. Motta, L. and Faúndes N. "Active / passive harmonic filters: applications, challenges & trends", *17th International Conference on Harmonics and Quality of Power (ICHQP)*, pp. 657–662 (2016).
2. Ochoa-Giménez, M., García-Cerrada, A., and Zamora-Macho, J. "Comprehensive control for unified power quality conditioners", *Journal of Modern Power Systems and Clean Energy*, **5**(4), pp. 411–416 (2017).
3. Bhosale, S.S., Bhosale, Y.N., Chavan, U.M., et al. "Power quality improvement by using UPQC: A review", *2018 International Conference on Control, Power, Communication and Computing Technologies (ICCPCCT)*, pp. 375–380 (2018).
4. Yu, J. , Xu, Y., and Li, Y. "An inductive hybrid UPQC for power quality management in premium-power-supply-required applications", *IEEE Access*, **8**, pp. 113342–113354 (2020).
5. Wang, L., Lam, C., and Wong, M. "Hybrid structure of static var compensator and hybrid active power filter (SVC//HAPF) for medium-voltage heavy loads compensation", *IEEE Transactions on Industrial Electronics*, **65**(6), pp. 4432–4442 (2018).
6. Saidi, S., Abbassi, R., and Chebbi, S. "Virtual flux based direct power control of shunt active filter", *Scientia Iranica*, D, **21**(6), pp. 2165–2176 (2014).
7. Tey, L.H., So, P.L., and Chu, Y.C. "Improvement of power quality using adaptive shunt active filter", *IEEE Trans. Power Del.*, **20**, pp. 1558–1568 (2005).
8. Anu, G. and Fernandez, F.M. "Identification of harmonic injection and distortion power at customer location", *19th International Conference on Harmonics and Quality of Power (ICHQP)*, pp. 1–5 (2020).
9. Li, D., Yang, K., Zhu, Z.Q., et al. "A novel series power quality controller with reduced passive power filter", *IEEE Transactions on Industrial Electronics*, **64**(1), pp. 773–784 (2017).
10. Mehri, R. and Mokhtari, H. "Harmonic effects optimization at a system level using a harmonic power flow controller", *Turkish Journal of Electrical Engineering & Computer Sciences*, **28**, pp. 2586–2601 (2020).
11. Zhang, S. and Zhao, Z. "Control strategy for dynamic voltage restorer under distorted and unbalanced voltage conditions", *IEEE International Conference on Industrial Technology (ICIT)*, Melbourne, VIC, Australia (2019).
12. Meisner, D., Niemann, B., and Shevchenko, M. "STATCOM with active filter using STATCOM as active filter, improving power quality and reducing harmonics", *IEEE/PES Transmission and Distribution Conference and Exposition (T&D)*, Chicago, IL, USA (2020).
13. HAN, xio, M., You, Y., et al. "Principle and realization of a dynamic voltage regulator (DVR) based on line voltage compensating", *Proceedings of the CSEE 12* (2003).
14. Ghosh, A. and Ledwich, G. "Structures and control of a dynamic voltage regulator (DVR)", *Power Engineering Society Winter Meeting 2001*, IEEE, **3**, pp. 1027–1032 (2001).
15. Yuan, X., Huang, X., and Guo, L. "Implementation of a control strategy for harmonic suppression and dynamic voltage compensation in series active power filter", *23rd International Conference on Electrical Machines and Systems (ICEMS)*, Hamamatsu, Japan (2020).
16. Ribeiro, E.R. and Barbi, I. "Harmonic voltage reduction using a series active filter under different load conditions", *IEEE Trans. Power Electronics*, **21**, pp. 1394–1402 (2006).
17. Transmission & Distribution Committee IEEE Power Engineering Society "Test systems for harmonics modeling and simulation", *IEEE Transactions on Power Delivery*, **14**(2), pp. 579–587 (1999).
18. Mena Kodsi, S.K. and Canizares, C.A. "Modeling and simulation of IEEE 14 bus system with facts controllers", University of Waterloo, Canada, Tech. Rep. (2003).

Biographies

Reza Mehri received the BSc degree (top degree) in electrical engineering from Shiraz University, Shiraz, Iran, in 1999 and the MSc degree (top degree) in electrical engineering from the Isfahan University of Technology (IUT), Isfahan, Iran, in 2002. He is currently pursuing a PhD degree in the Department of Engineering, College of Electrical Engineering, Tehran Science and Research Branch, Islamic Azad University, Tehran, Iran. In 2002, he joined the Department of Electrical Engineering, College of Islamic Azad University branch of Hamedan. His fields of interest include Power Quality, Power system Reliability and Protection, and Renewable Energy Sources.

Hossein Mokhtari was born in Tehran, Iran, on August 19, 1966. He received a BSc degree in electrical engineering from Tehran University, Tehran, in 1989. He received the MSc degree in power electronics from the University of New Brunswick, Fredericton, NB, Canada, in 1994 and the PhD degree in power electronics/power quality from the University of Toronto, Toronto, Canada, in 1999. From 1989 to 1992, he worked in the Consulting Division of Power Systems Dispatching Projects, Electric Power Research Center Institute, Tehran. Since 2000, he has been with the Department of Electrical Engineering, Sharif University of Technology, Tehran, where he is currently a Professor.

He is also a Senior Consultant to several utilities and industries.

Mohammad Reza Zolghadri is an Associate Professor and the Head of the Power System Group at the Department of Electrical Engineering, Sharif University of Technology, Tehran, Iran. He received his BSc and MSc degrees from Sharif University of Technology in 1989 and 1992, respectively, and a PhD degree from the Institute National Poly Technique de Grenoble, Grenoble, France, in 1997, all in Electrical Engineering. In 1997, he joined the Department of Electrical Engineering of Sharif University of Technology. From 2000 to 2003, he was a Senior Researcher in the Electronics Laboratory of SAM Electronics Company, Tehran. From 2003 to 2005, he was a Visiting Professor at North Carolina A&T State University, USA. He is the Founder and Head of the Electric Drives and Power Electronics Lab (EDPEL) at the Sharif University of Technology. He is a member of the founding board of the Power Electronics Society of Iran (PESI). He is the author of more than 100 publications in power electronics and variable speed drives. His fields of interest are the application of power electronics in energy systems, variable speed drives, and modeling and control of power electronic converters.